Quantum chaos and order based on classically moving reference frames

Wenhua Hai,[1,2,*] Qiongtao Xie,[1] and Jianshu Fang[1]
[1]*Department of Physics, Hunan Normal University, Changsha 410081, China*
[2]*Department of Physics, Jishou University, Jishou 416000, Hunan, China*
(Received 2 April 2005; published 26 July 2005)

We develop a mathematically consistent approach for treating the quantum systems based on moving classical reference frames. The classical and quantum exact solutions show excellently classical-quantum correspondence, in which the quantum chaotic coherent states correspond to the classically chaotic motions. Applying the approach to the periodically driven linear and nonlinear oscillators, the regular and chaotic quantum states and quantum levels, and the quantum chaotic regions are evidenced. The results indicate that chaos may cause the collapse of matter wave packets and suppress the quantum effect of energy.

DOI: 10.1103/PhysRevA.72.012116 PACS number(s): 03.65.Ca, 05.45.Ac, 03.65.Ge, 05.45.Mt

I. INTRODUCTION

In 1905, Einstein proposed the well-known principle of relativity [1]; that is, the laws of physics are the same in different inertial reference frames. Here both the physical systems and their reference frames are classical. In quantum mechanics, a problem has arisen, how do the physical laws change if the considered systems are quantum and the reference frames are classical? Quantum measurement based on the classical reference frame is the basis of quantum mechanics. In many quantum treatments, only the motionless classical reference frames are considered. When the reference frame moves obeying the classical-mechanical law, the interaction between macroscopic and microscopic systems will induce the coupling between them. The macroscopic-microscopic coupled systems are a kind of general systems in any laboratory, where the microscopic systems may be some atoms, molecules and photons, or say the corresponding very weak fields in macroscopic viewpoint. Some experimentally interesting examples of them are the microscopic systems on the surfaces of moving macroscopic systems or the microscopic systems probed by the macroscopically moving detectors.

Usually, the macroscopic and microscopic systems are described by the classical variables and the quantum ones, respectively. In the viewpoints of quantum mechanics [2,3], the quantum variables can also be used to explore the macroscopic systems through their classical limits. But the classical variables cannot be employed for treating the microscopic systems, except for the semiclassical description [4]. The classical limit of quantum mechanics leads to a route to an important principle, the classical-quantum correspondence (CQC). However, a serious problem has arisen in the fully quantum-mechanical treatments for the classically chaotic systems, that is the breakdown of the correspondence principle [5–7].

The quantum dynamics of classically chaotic systems has been a subject of considerable interest in recent years [8,9]. The usual definition on classical chaos emphasizes the sensitive dependence of phase-space trajectories on the initial conditions and resists direct transition to quantum mechanics, since quantum mechanics admits wave functions and does not admit the classical trajectories [10,11]. Hence, investigating the CQC on chaotic behaviors cannot rely upon the standard formulations of quantum and classical mechanics. Fortunately, the correspondence between a classical particle and a quantum Gaussian wave packet has been demonstrated as a good scheme, which can be realized by a harmonic oscillator of coherent states [12–14] with the quantum wave packet propagating along the classical trajectory. The result was extended to the generalized harmonic oscillators with time-dependent frequencies [15–18]. On the other hand, we have suggested a method to construct the classically chaotic solutions [19] of the linearized equations for the nonlinear weak chaotic systems [20,21]. This method has also been applied to several different physical systems and resulted in some interesting results [22]. Apparently, the linearized systems of the original systems are just a kind of generalized harmonic oscillators. This supplies a route to CQC between the classical chaos in the linearized systems and the irregular motions of the quantum wave packet for the generalized harmonic oscillators.

Recently, the classical-quantum coupled systems have attracted significant interests [23,24]. The coupling between a quasiclassical variable and a quantum one was phenomenologically described by using the variational principle and the theory of continuous quantum measurement [25,26]. The mixed quantum-classical treatments were applied in many different areas [27,28]. In this paper, we shall present a mathematically consistent approach for treating the quantum systems based on classically moving reference frames. Utilizing a direct perturbation theory, we separate the combined system of the macroscopic frame with microscopic field into n subsystems and identify the zero-order and first-order subsystems as the classical and quantum ones, respectively. That is, the leading order subsystem obeys classical dynamics, but its first-order correction obeys quantum mechanics. Applying the approach to the systems of weakly driven linear and nonlinear oscillators, we find excellent CQC in chaos, in which the quantum chaotic coherent states correspond to the classically chaotic solutions. The classical and quantum exact

*Corresponding author. Electronic address: whhai2005@yahoo.com.cn

solutions of the microscopic subsystems reveal many interesting properties such as the classical and quantum chaotic states, the regular and chaotic quantum levels, and the quantum chaotic regions.

The outline of this paper is as follows. We present the approach for separating the macroscopic-microscopic coupled systems in the next section. In Sec. III, we propose the general CQC protocol of the microscopic subsystem, that is valid for both the regular and chaotic systems. The approach and protocol are applied to the systems of a periodically driven linear oscillator and a nonlinear Duffing system, respectively, in Sec. IV and Sec. V. Last, we briefly summarize the results and discuss some challenging topics.

II. SEPARATION OF THE COUPLED SYSTEM

In order to study a microscopic system on the surface of a macroscopically moving system, say a flight simulator, or to probe a microscopic system by employing a macroscopically moving detector, one must consider the coupling between the macroscopic and microscopic systems. For a general macroscopic-microscopic coupled system, its dynamics is dominated by the Hamiltonian

$$H = \frac{p^2}{2m} + V_0(r,t) + \lambda V_1(r,t), \tag{1}$$

where V_0 denotes the macroscopic potential governing the classical reference frame, V_1 is the interaction potential with strength $|\lambda| \ll 1$ being of the microscopic order, which may result from some atoms, molecules, and photons. According to the viewpoint of quantum mechanics, the system including the microscopic subsystem cannot be treated by using classical mechanics. In the fully quantum-mechanical treatment, the macroscopic-microscopic coupled system is usually unsolvable that necessitates the quantum perturbation theory [29–31]. However, if the system (1) is a classically chaotic one, the fully quantum-mechanical treatment may lead to a breakdown of the correspondence principle [5–7]. In order to seek the CQC for the chaotic systems, one had to employ some semiclassical approximate methods [32,33]. In this section we shall adopt the classical perturbation theory to separate such coupled systems into a completely classical system and a pure quantum one that supplies a mathematically consistent procedure for investigating the considered problems.

For simplicity, we only consider the one-dimensional case of Eq. (1). The classical canonical equations of motion $\dot{x} = \partial H/\partial p, \dot{p} = -\partial H/\partial x$ are equivalent to the second order equation

$$m\ddot{x} = -\frac{\partial}{\partial x}[V_0(x,t) + \lambda V_1(x,t)]. \tag{2}$$

Using the direct perturbation method, we first expand the coordinate variable as

$$x = x_0 + \sum_{i=1}^{\infty} x_i \tag{3}$$

with x_i in the order of λ^i. Therefore, x_0 represents the macroscopic variable of the classical reference frame, x_1 is a microscopic quantity being proportional to the perturbation parameter λ, and x_i for $i > 1$ are the infinitesimals of $i \geqslant 2$ orders which will be neglected in the latter. Near x_0, one can expand $V_0(x,t)$ as $V_0(x_0,t) + (\partial V_0/\partial x_0)x_1 + \cdots$. Inserting this expansion and Eq. (3) into Eq. (2) and comparing the terms of same order in both sides, one can obtain the zero-order equation

$$m\ddot{x}_0 = -\frac{\partial}{\partial x_0} V_0(x_0,t) \tag{4}$$

for the classical reference frame and the first-order equation

$$m\ddot{x}_1 = -V_0''(t)x_1 - \lambda V_1'(t) \tag{5}$$

for the quantum subsystem. Here, $V_0''(t) = \partial^2 V_0/\partial x_0^2 = V_0''[x_0(t),t], V_1'(t) = \partial V_1/\partial x_0 = V_1'[x_0(t),t]$. The system dominated by Eq. (4) is a Hamilton's one with the Hamiltonian

$$H_0 = \frac{p_0^2}{2m} + V_0(x_0,t), \tag{6}$$

where p_0 is the conjugate momentum of the canonical coordinate x_0. The Hamilton system (6) is independent of the perturbation parameter λ and the microscopic variable x_1, so it is a pure macroscopic system and can be solved directly by the classical law of motion. Applying the zero-order solution $x_0(t)$ of Eq. (4) to Eq. (5), the latter becomes a linearized equation with the variable coefficient $-V_0''(t)$ and nonhomogeneous term $-\lambda V_1'(t)$. When Eq. (4) is a nonlinear system, the coefficient of Eq. (5) depends on the classical solution $x_0(t)$, and the linear equation (4) leads the coefficient of Eq. (5) to be independent of $x_0(t)$.

Replacing the macroscopic coordinate x_0 with its time-dependent classical solution $x_0(t)$, the spatial variable in Eq. (5) is only the microscopic one x_1. Therefore, the system governed by Eq. (5) is a pure microscopic one that should be treated by employing quantum mechanics. To quantize the microscopic subsystem (5), we construct the corresponding Hamiltonian operator

$$H_1 = \frac{p_1^2}{2m} + \frac{1}{2}V_0''(t)x_1^2 + \lambda V_1'(t)x_1, \tag{7}$$

with $p_1 = -i\hbar\partial/\partial x_1$ denoting the conjugate momentum of x_1. Obviously, the canonical equations $\dot{x}_1 = \partial H_1/\partial p_1$ and $\dot{p}_1 = -\partial H_1/\partial x_1$ are equivalent to the equation of motion (5). The quantum dynamics of the linearized system (5) is dominated by the Schrödinger equation [2,3]

$$i\hbar\frac{\partial\psi(x_1,t)}{\partial t} = H_1\psi(x_1,t) \tag{8}$$

with wave function $\psi(x_1,t)$. Thus we have separated the coupled macroscopic-microscopic system (1) into the macroscopic subsystem (6) and microscopic subsystem (7). The former is governed by only the classical equation (4) and the latter is dominated by both the classical equation (5) and the quantum one (8). Clearly, the former play the role of a moving reference frame for the latter. It is worth noting that Eq. (8) completely differs from the perturbed equation in the

previous quantum perturbation theory. Particularly, Eqs. (1), (6), and (7) mean that $H \neq H_0 + H_1$ in our theory.

III. CLASSICAL-QUANTUM CORRESPONDENCE

We are interested in the CQC of the microscopic subsystem (7). It is easy to solve the linearized nonhomogeneous equation (5). Utilizing the techniques of constant variation and the natural units, the general solutions of Eq. (5) in classical phase space can be expressed as [19]

$$x_{1c}(t) = A\phi_1(t) + B\phi_2(t) + \lambda\left(\phi_1(t)\int_0^t \phi_2(t)V_1'(t)dt - \phi_2(t)\int_0^t \phi_1(t)V_1'(t)dt\right),$$

$$p_{1c}(t) = A\dot{\phi}_1(t) + B\dot{\phi}_2(t) + \lambda\left(\dot{\phi}_1(t)\int_0^t \phi_2(t)V_1'(t)dt - \dot{\phi}_2(t)\int_0^t \phi_1(t)V_1'(t)dt\right), \quad (9)$$

where $\phi_1(t)$ and $\phi_2(t) = \phi_1 \int (\phi_1)^{-2} dt$ denote the two linearly independent solutions of the Eq. (5) with $\lambda = 0$, A and B are two arbitrary constants determined by the classical initial conditions of the system, and the terms proportional to λ represent a special solution of Eq. (5). If Eq. (4) is a nonlinear equation, $\phi_i(t)$ is related to its solution $x_0(t)$. Further if $x_0(t)$ is a homoclinic or heteroclinic solution [21] and $V_1'(t)$ is a time-periodic function, Eq. (9) is just the chaotic solution [22] under the Melnikov's chaos criterion [20].

Now, we begin to seek the relationship between the classical solutions Eq. (9) and the quantum wave function in Eq. (8). We have known the similar relationship for the time-dependent harmonic system (7) with $\lambda = 0$ [15–17]. Applying the Husimi's test-function method [34] and using the natural units with $m = \hbar = 1$, we take the solution of Eq. (8) in the form

$$\psi_n(x,t) = a_n(t)H_n(\xi)e^{[b(t)x_1 - c(t)x_1^2 - f^2(t)/2]},$$

$$\xi = e(t)x_1 - f(t), \quad n = 0, 1, \ldots . \quad (10)$$

Here $a_n(t), b(t), c(t)$ are the complex functions of time and $e(t), f(t)$ the real functions, and $H_n(\xi)$ the Hermitian polynomial of variable ξ. Taking the first-order partial derivative with respect to time and the second one with respect to coordinate from Eq. (10) results in

$$i\frac{\partial \psi_n}{\partial t} = ia_n\left(\frac{\dot{a}_n}{a_n}H_n + (\dot{e}x_1 - \dot{f})\frac{\partial H_n}{\partial \xi} + (\dot{b}x_1 - f\dot{f} - \dot{c}x_1^2)H_n\right)e^{[b(t)x_1 - c(t)x_1^2 - f^2(t)/2]},$$

$$\frac{\partial^2 \psi_n}{\partial x_1^2} = a_n\left(e^2\frac{\partial^2 H_n}{\partial \xi^2} + (2b - 4cx_1)e\frac{\partial H_n}{\partial \xi} + (b^2 - 2c - 4bcx_1 + 4c^2x_1^2)H_n\right)e^{[b(t)x_1 - c(t)x_1^2 - f^2(t)/2]}.$$

Applying these and Eq. (7) to Eq. (8), we arrive at the equation

$$e^2\frac{\partial^2 H_n}{\partial \xi^2} + 2(be - i\dot{f} + i\dot{e}x_1 - 2cex_1)\frac{\partial H_n}{\partial \xi} + 2\left[i\frac{\dot{a}_n}{a_n} - if\dot{f} + \frac{b^2}{2} - c + [i\dot{b} - 2bc - \lambda V_1'(t)]x_1 + \left(2c^2 - i\dot{c} - \frac{1}{2}V_0''(t)\right)x_1^2\right]H_n = 0. \quad (11)$$

Notice that the Hermitian polynomial must obey the Hermitian equation $\partial^2 H_n/\partial \xi^2 - 2\xi \partial H_n/\partial \xi + 2nH_n = 0$. Comparing this with Eq. (11) yields

$$i\dot{c} = 2c^2 - V_0''(t)/2, \quad i\dot{b} = 2bc + \lambda V_1'(t), \quad i\dot{e} = 2ce - e^3,$$

$$i\dot{f} = be - e^2 f, \quad i\dot{a}_n/a_n = if\dot{f} - b^2/2 + c + ne^2. \quad (12)$$

This group of equations is similar to Eq. (4) of Ref. [16] and Eq. (5) of Ref. [35], when $\lambda = 0$ is set. Adopting the same method with Refs. [16,35] we can easily derive its formally exact solution as follows.

The first of Eq. (12) is a complex Riccati equation, which can be transformed into a complex equation of a classical harmonic oscillator with time-dependent frequency,

$$\ddot{\varphi} = -V_0''(t)\varphi, \quad (13)$$

through the function transformation $c = \dot{\varphi}/(2i\varphi)$. The general solution of Eq. (13) can be easily found as

$$\varphi = \varphi_1 + i\varphi_2 = \rho(t)\exp[i\theta(t)], \quad (14)$$

where the real functions φ_1 and φ_2 are the real and imaginary parts of φ. We will use φ_i, ρ, and θ in Eq. (14) as the known functions throughout the paper. Comparison between Eq. (13) with Eq. (5) shows that Eq. (13) has the form of the homogenous equation of Eq. (5) with $\lambda = 0$. However, the solutions of Eq. (13) can be some complex functions and Eq. (5) has only real solutions physically. Given the two linearly independent solutions of the homogeneous equation ϕ_i as in Eq. (9), the real function φ_i reads

$$\varphi_i = C_i\phi_1 + D_i\phi_2, \quad (15)$$

where C_i and D_i are arbitrary real constants adjusted by the initial conditions of the classical harmonic oscillator, and the real functions $\rho(t)$ and $\theta(t)$ obey

$$\rho = \sqrt{\varphi_1^2 + \varphi_2^2} = \sqrt{(C_1\phi_1 + D_1\phi_2)^2 + (C_2\phi_1 + D_2\phi_2)^2},$$

$$\theta = \arctan\frac{\varphi_2}{\varphi_1} = \arctan\frac{C_2\phi_1 + D_2\phi_2}{C_1\phi_1 + D_1\phi_2}. \quad (16)$$

Given the function φ, the transformation between it and c gives

$$c = \frac{\dot{\varphi}}{2i\varphi} = \frac{1}{2}\dot{\theta} - i\frac{\dot{\rho}}{2\rho}. \tag{17}$$

Substituting Eq. (14) into Eq. (13) yields the equations of the amplitude and phase as

$$\ddot{\theta} = -2\dot{\theta}\dot{\rho}/\rho, \quad \ddot{\rho} = \rho\dot{\theta}^2 - V_0''(t)\rho \tag{18}$$

with the first integration constant

$$c_0 = \rho^2\dot{\theta} = \varphi_1\dot{\varphi}_2 - \varphi_2\dot{\varphi}_1, \tag{19}$$

which equates the Wronskian constant. Given the function $c(t)$ as in Eq. (17), from equation group (12) we can easily obtain the complex functions $a(t), b(t)$ and real functions $e(t), f(t)$. At first we insert Eq. (17) into the second equation of Eq. (12) and apply the constant-variation method, producing

$$\begin{aligned} b(t) &= b'(t) + ib''(t) \\ &= \varphi^{-1}\left(b_0 - i\lambda\int_0^t V_1'(t)\varphi dt\right) \\ &= \frac{\varphi_1 - i\varphi_2}{\rho^2}\left(b_0' + ib_0'' - i\lambda\int_0^t V_1'(t)(\varphi_1 + i\varphi_2)dt\right), \end{aligned}$$

$$b'(t) = \frac{\varphi_1}{\rho^2}\left(b_0' + \lambda\int_0^t V_1'(t)\varphi_2 dt\right) + \frac{\varphi_2}{\rho^2}\left(b_0'' - \lambda\int_0^t V_1'(t)\varphi_1 dt\right),$$

$$b''(t) = \frac{\varphi_1}{\rho^2}\left(b_0'' - \lambda\int_0^t V_1'(t)\varphi_1 dt\right) - \frac{\varphi_2}{\rho^2}\left(b_0' + \lambda\int_0^t V_1'(t)\varphi_2 dt\right). \tag{20}$$

Here b_0' and b_0'' are two real constants related to the initial conditions, and $b'(t), b''(t)$ are two real functions. Noticing that $e(t)$ is a real function and applying Eqs. (17) and (19) to the third equation of Eq. (12), we get

$$\frac{\dot{e}}{e} = -\frac{\dot{\rho}}{\rho}, \quad e = \pm\sqrt{\dot{\theta}} = \pm\frac{\sqrt{c_0}}{\rho}. \tag{21}$$

Similarly, because $f(t)$ is a real function and $b(t)$ in Eq. (20) is a complex function, the fourth equation of Eq. (12) and Eq. (21) give

$$\dot{f} = eb'' = \pm\sqrt{c_0}\frac{b''}{\rho}, \quad f = \frac{b'}{e} = \pm\frac{b'\rho}{\sqrt{c_0}}. \tag{22}$$

This implies the relationship $(d/dt)(b'\rho)/\sqrt{c_0} = \sqrt{c_0}b''/\rho$, which is just satisfied by Eq. (20). In fact, with $\varphi_1/\rho = \cos\theta$, $\varphi_2/\rho = \sin\theta$, and $\dot{\theta} = c_0/\rho^2$, from Eq. (20) we can immediately obtain this relationship. The final equation of Eq. (12) seems to be complicated, whose solution can be constructed by the direct integration

$$a = a_n = A_n \exp\left[\frac{f^2}{2} + i\int\left(\frac{b^2}{2} - c - ne^2\right)dt\right], \tag{23}$$

where A_n is a normalization constant. Noticing $b^2 = b'^2 - b''^2 + 2ib'b''$ and Eq. (22), we have the integration $\int b'b''dt = \int f df = f^2/2$. Substituting this and Eqs. (17) and (21) into Eq. (23) leads to

$$a_n = \frac{A_n}{\sqrt{\rho}}\exp\left\{-i\left[\left(\frac{1}{2} + n\right)\theta - \frac{1}{2}\int(b'^2 - b''^2)dt\right]\right\} \tag{24}$$

in terms of the real functions $\rho(t)$, $\theta(t)$, $b'(t)$, and $b''(t)$. It is interesting that by Eqs. (17), (21), and (22) we mean

$$\begin{aligned} b(t)x_1 - c(t)x_1^2 - \frac{f^2(t)}{2} &= \left(b'x_1 - \frac{\dot{\theta}}{2}x_1^2 - \frac{f^2}{2}\right) + i\left(b''x_1 + \frac{\dot{\rho}}{2\rho}x_1^2\right) \\ &= \left(efx_1 - \frac{e^2}{2}x_1^2 - \frac{f^2}{2}\right) + i\left(b''x_1 + \frac{\dot{\rho}}{2\rho}x_1^2\right) \\ &= -\frac{1}{2}\xi^2 + i\left(b''x_1 + \frac{\dot{\rho}}{2\rho}x_1^2\right), \end{aligned}$$

where $\xi = ex_1 - f$, as in Eq. (10). Applying this and Eq. (24) to Eq. (10) produces the orthonormalized exact wave function

$$\psi_n(x_1,t) = R_n(x_1,t)\exp[i\Theta_n(x_1,t)],$$

$$R_n(x_1,t) = \frac{(c_0/\pi)^{1/4}}{\sqrt{2^n n!\rho(t)}}H_n(\xi)\exp\left(-\frac{1}{2}\xi^2\right),$$

$$\Theta_n(x_1,t) = b''(t)x_1 + \frac{\dot{\rho}(t)}{2\rho(t)}x_1^2 - \left(\frac{1}{2} + n\right)\theta(t) + \frac{1}{2}\int[b'^2(t) - b''^2(t)]dt,$$

$$\xi = \frac{\sqrt{c_0}}{\rho(t)}x_1 - \frac{\rho(t)}{\sqrt{c_0}}b'(t), \quad n = 0,1,2,\ldots. \tag{25}$$

Here the normalization condition $\int|\psi_n|^2dx_1 = A_n^2\sqrt{c_0^{-1}}\int H_n^2(\xi)\exp(-\xi^2)d\xi = A_n^2\sqrt{\pi c_0^{-1}}2^n n! = 1$ has been used to give the normalization constant $A_n = [\sqrt{c_0}/(\sqrt{\pi}2^n n!)]^{1/2}$. In Eq. (25), the function $\rho(t)$ and $\theta(t)$ depend on the macroscopic potential $V_0[x_0(t),t]$ through Eqs. (13) and (14), and Eq. (20) shows the correlation of the functions $b'(t)$ and $b''(t)$ to the microscopic potential $V_1[x_0(t),t]$.

In Eqs. (15), (19), and (20), more arbitrary constants are introduced for the quantum solution (25), but only two arbitrary constants are needed in the classical solution (9). These constants may not be independent and there exist some relations between C_i, D_i, and c_0. For example, combining Eqs. (15), (16), and (19), and noticing the Wronskian constant $\dot{\phi}_2\phi_1 - \dot{\phi}_1\phi_2 = 1$, we find one of the relations

$$\begin{aligned} c_0 &= \dot{\varphi}_2\varphi_1 - \dot{\varphi}_1\varphi_2 \\ &= (C_1D_2 - C_2D_1)(\dot{\phi}_2\phi_1 - \dot{\phi}_1\phi_2) = C_1D_2 - C_2D_1. \end{aligned}$$

However, there have four independent constants associated with $c(t)$ and $b(t)$, since the equations governing them are complex ones in Eq. (12), which contain four independent integration constants. Hence the quantum solution (25) includes more independent constants and more choices of

states than the classical Eq. (9). We now seek the interesting kind of these quantum states, the coherent state, through the selections of the arbitrary constants. The Schrödinger's original definition [12–14] of the coherent state ψ_n requires $x_{1c}=x_{1q}$, $p_{1c}=p_{1q}$ with $(x_{1q}=\langle\psi_n|x_1|\psi_n\rangle, p_{1q}=\langle\psi_n|p_1|\psi_n\rangle)$ being the quantum expectation values of (x_1,p_1). Noticing the orthonormalization condition $\langle\psi_n|\psi_{n'}\rangle=\delta_{nn'}$ and the formulas

$$\xi\psi_n=\sqrt{n/2}\psi_{n-1}e^{-i\theta}+\sqrt{(n+1)/2}\psi_{n+1}e^{i\theta},$$

$$2\xi^2\psi_n=\sqrt{n(n-1)}\psi_{n-2}e^{-2i\theta}+(2n+1)\psi_n+\sqrt{(n+1)(n+2)}\psi_{n+2}e^{2i\theta},$$

$$\frac{1}{H_n}\frac{\partial H_n}{\partial\xi}\psi_n=2n\frac{H_{n-1}}{H_n}\psi_n=\sqrt{2n}\psi_{n-1}e^{-i\theta}, \tag{26}$$

from Eqs. (25), (22), and (20) we immediately obtain

$$\begin{aligned}x_{1q}(t)&=\langle\psi_n|x_1|\psi_n\rangle\\&=\frac{\rho^2}{c_0}b'=\frac{\varphi_1}{c_0}\left(b_0'+\lambda\int_0^t V_1'(t)\varphi_2dt\right)+\frac{\varphi_2}{c_0}\left(b_0''-\lambda\int_0^t V_1'(t)\varphi_1dt\right),\end{aligned}$$

$$\begin{aligned}p_{1q}(t)&=\langle\psi_n|-i\frac{\partial}{\partial x_1}|\psi_n\rangle\\&=b''+\frac{\dot\rho}{\rho}x_{1q}\\&=b''+\frac{\dot\rho\rho}{c_0}b'\\&=\frac{2\dot\rho\rho}{c_0}b'+\frac{\rho^2}{c_0}\dot b'\\&=\dot x_{1q}=\frac{\dot\varphi_1}{c_0}\left(b_0'+\lambda\int_0^t V_1'(t)\varphi_2dt\right)+\frac{\dot\varphi_2}{c_0}\left(b_0''-\lambda\int_0^t V_1'(t)\varphi_1dt\right).\end{aligned} \tag{27}$$

When the constants C_i and D_i of Eq. (15) are selected as $C_1=D_2=\sqrt{c_0}$, $C_2=D_1=0$, Eq. (15) becomes

$$\varphi_1=\sqrt{c_0}\phi_1,\quad \varphi_2=\sqrt{c_0}\phi_2. \tag{28}$$

Applying them to Eq. (27) and setting $b_0'/\sqrt{c_0}=A$, $b_0''/\sqrt{c_0}=B$ lead Eq. (27) to the same form with Eq. (9), namely $(x_{1q},p_{1q})=(x_{1c},p_{1c})$. In other words, the definition of coherent state makes the numbers of independent constants to reduce to 2, namely only the classical constants A and B of Eq. (9) are required in the quantum-mechanical coherent state included in Eq. (25).

The norm $R_n^2(x_1,t)$ of exact solution (25) for any quantum number n describes the wave packet train consisting of $n+1$ packets at any time, since it is proportional to the Hermitian polynomial $H_n^2(\xi)$. The instantaneous ground state with $n=0$ is a Gaussian wave packet similar to that of the coherent state of a harmonic oscillator [12–14]. The function $\rho(t)$ that appears in ξ of R_n describes the widths of the wave packet train and each packet. For any train the average width of the packets is $\rho/\sqrt{c_0}$. The same function that appears in the radical of equation (25) determines the heights of every packet. When the changes in the widths and heights are small, the wave packets agree approximately with a propagating train without deformation. The normalization condition implies that the broader wave packet train associates with smaller mean height, and the narrower wave packet train corresponds to larger mean height. The orbit of the center of the wave packet train is given as $x_1=x_c(t)$ from $\xi=0$. Applying Eqs. (20)–(22) and (27), from $\xi=0$ we have the center orbit

$$x_c(t)=\frac{f}{e}=\frac{b'}{e^2}=\frac{\rho^2}{c_0}b'=x_{1q}(t)=x_{1c}(t). \tag{29}$$

This means that in the considered case the center of the quantum wave packets moves along the corresponding classical orbit. Thus under the condition (28) we arrive at a good CQC in the microscopic subsystem. Therefore, we can assert that Eq. (28) is also the requirement of the correspondence principle. This CQC is valid for the classical chaotic systems with $x_{1c}(t)$ being the chaotic solution [22] under the Melnikov's chaos criterion, since the corresponding quantum wave packets propagate along the chaotic orbit, $x_c(t)=x_{1c}(t)$, and the quantum-mechanical expectation orbit is also the chaotic one, $x_{1q}(t)=x_{1c}(t)$.

The phase of wave function $\Theta_n(x_1,t)$ is a complicated temporal-spatial function, which is directly related to the energy of the microscopic subsystem. Applying Eqs. (25)–(27) to calculate the expectation value of energy, we obtain

$$E_n(t)=\langle\psi_n|i\frac{\partial}{\partial t}|\psi_n\rangle=\langle\psi_n|\left(i\frac{\dot R_n}{R_n}-\dot\Theta_n\right)|\psi_n\rangle$$

The imaginary part vanishes, because of the equation

$$\begin{aligned}\langle\psi_n|\frac{\dot R_n}{R_n}|\psi_n\rangle&=-\frac{i\dot\rho}{2\rho}+i\ \psi_n|\dot\xi\left(\frac{1}{H_n}\frac{\partial H_n}{\partial\xi}-\xi\right)|\psi_n\rangle\\&=-\frac{i\dot\rho}{2\rho}-i\langle\psi_n|\sqrt{2n}\frac{\dot\rho}{\rho}\xi|\psi_{n-1}\rangle+i\langle\psi_n|\frac{\dot\rho}{\rho}\xi^2|\psi_{n-1}\rangle=0,\end{aligned}$$

where Eqs. (25) and (26), and $\dot\xi=x\dot e-\dot f=-\dot\rho(\xi+f)/\rho-\dot f$ have been used. Given this equation, the real energy becomes

$$\begin{aligned}E_n(t)&=-\langle\psi_n|\dot\Theta_n|\psi_n\rangle\\&=\left(\frac{1}{2}+n\right)\dot\theta-\frac{1}{2}(b'^2-b''^2)-\dot b''x_{1c}-\frac{d}{dt}\left(\frac{\dot\rho}{2\rho}\right)\langle\psi_n|\left(\frac{\rho^2}{c_0}\xi^2+\frac{\rho^4}{c_0^2}b'^2\right)|\psi_n\rangle\\&=\left(\frac{1}{2}+n\right)\left[\frac{c_0}{\rho^2}-\frac{\rho^2}{c_0}\frac{d}{dt}\left(\frac{\dot\rho}{2\rho}\right)\right]-\frac{1}{2}(b'^2-b''^2)-\dot b''x_{1c}\end{aligned}$$

$$-\frac{d}{dt}\left(\frac{\dot{\rho}}{2\rho}\right)x_{1c}^2.$$

From Eqs. (27) and (22) we get $b'=\rho^2 x_{1c}/c_0$, $b''=p_{1c}-\dot{\rho}x_{1c}/\rho$. Applying them and Eqs. (5), (18), and (19) to the energy formula yields

$$E_n(t)=\left(\frac{1}{2}+n\right)\frac{1}{2c_0}\left(\frac{c_0^2}{\rho^2}+\dot{\rho}^2+V_0''(t)\rho^2\right)+\frac{1}{2}[p_{1c}^2+V_0''(t)x_{1c}^2]+\lambda V_1'(t)x_{1c}. \tag{30}$$

Here the functions ρ, $x_{1c}=x_{1q}$ and $p_{1c}=p_{1q}$ are shown in Eqs. (16) and (27). It is very interesting noting that the expectation value of energy consists of the classical energy as in Eq. (7) and the quantum level. In the case $V_0''=$constant, $\frac{1}{2}(c_0^2/\rho^2+\dot{\rho}^2+V_0''\rho^2)$ is just one of the first integration constants of Eq. (18). Thus for the time-independent Hamiltonian with $V_0''=$constant and $V_1'=$constant, the quantum level becomes the well-known level of a stationary state harmonic oscillator. In the viewpoint of quantum mechanics, the system can transit between the different energy states with different quantum number n.

IV. EXACT QUANTUM MOTION OF A DRIVEN OSCILLATOR

To evidence the above-mentioned results, we now take a macroscopic harmonic oscillator driven by a microscopic periodic potential as a simple example. In the natural units with $m=\hbar=\omega=1$, the macroscopic and microscopic potential read

$$V_0(x_0)=\tfrac{1}{2}x_0^2,\quad \lambda V_1(x_0,t)=\lambda x_0\cos\nu t. \tag{31}$$

Consequently, the functions $V_0''(t)$, $V_1'(t)$ and the Hamiltonian of microscopic subsystem become

$$V_0''=1,\quad V_1'(t)=\cos\nu t,$$

$$H_1=\frac{p_1^2}{2}+\frac{1}{2}x_1^2+\lambda x_1\cos\nu t. \tag{32}$$

Here ω and ν are the harmonic frequency and driving frequency, respectively. Such linear oscillator has been experimentally realized by laser driving a Paul trapped ion [36]. Inserting Eqs. (31) and (32) into Eqs. (4) and (5), respectively, we obtain the zero order equation and the first order one. The homogenous equation associated with the latter is in the same form with the former. So they possess the same two linearly independent solutions as [22]

$$\phi_1=\sin t,\quad \phi_2=\phi_1\int(\phi_1)^{-2}dt=-\cos t. \tag{33}$$

The general solution of Eq. (4) is the linear superposition of the two solutions. The application of Eqs. (32) and (33) to the first of Eq. (9) gives the classical general solution of the nonhomogenous equation (5),

$$x_{1c}(t)=A\sin t-B\cos t+\lambda\left[\cos t\left(\frac{\cos[(\nu-1)t]-1}{2(\nu-1)}-\frac{\cos[(\nu+1)t]-1}{2(\nu+1)}\right)-\sin t\left(\frac{\sin[(\nu-1)t]}{2(\nu-1)}+\frac{\sin[(\nu+1)t]}{2(\nu+1)}\right)\right]. \tag{34}$$

The limits of $x_{1c}(t)$ at $\nu=\pm1(\omega)$ is called the resonance solution, which reads

$$x_{1,\nu=\pm1}(t)=\lim_{\nu\to\pm1}x_{1c}(t)=A\sin t-B\cos t+\frac{\lambda}{2}\left[\cos t\sin^2 t-\sin t\left(t+\frac{1}{2}\sin 2t\right)\right]. \tag{35}$$

The resonance solution contains the nonperiodical term $-\frac{1}{2}\lambda t\sin t$, which oscillates with amplitude being proportional to time t. With the increase of time, this will lead to loss of stability. In quantum mechanics, the resonance is associated with the quantum transitions between different states represented by the different quantum numbers.

Let us now derive the quantum-mechanical exact solution of the periodically driven harmonic oscillator from the given procedure. Combining Eq. (33) with Eq. (28), we get the CQC condition

$$\varphi_1=\sqrt{c_0}\sin t,\quad \varphi_2=-\sqrt{c_0}\cos t \tag{36}$$

for the considered system. Applying this to Eqs. (16), (17), (20)–(22), and (27) produces the solutions of Eq. (12) as

$$\rho=\sqrt{c_0},\quad \theta=t-\frac{\pi}{2},\quad c=\frac{1}{2},\quad e=\pm1,\quad f=\pm b' \tag{37}$$

and

$$b'=x_{1c}(t)=x_{1q}(t)=\langle\psi_n|x_1|\psi_n\rangle,$$

$$b''=B\sin t+A\cos t-\lambda\left[\sin t\left(\frac{\cos[(\nu-1)t]-1}{2(\nu-1)}-\frac{\cos[(\nu+1)t]-1}{2(\nu+1)}\right)-\cos t\left(\frac{\sin[(\nu-1)t]}{2(\nu-1)}+\frac{\sin[(\nu+1)t]}{2(\nu+1)}\right)\right], \tag{38}$$

$$a_n=\frac{1}{\sqrt{\sqrt{\pi}2^n n!}}\exp\left\{-i\left[\left(\frac{1}{2}+n\right)\left(t-\frac{\pi}{2}\right)-\frac{1}{2}\int(b'^2-b''^2)dt\right]\right\}, \tag{39}$$

where the formulas $b_0'/\sqrt{c_0}=A$, $b_0''/\sqrt{c_0}=B$ have been employed. Combining these with Eq. (25) leads to the amplitude and phase of the wave function,

$$R_n(x_1,t)=\frac{1}{\sqrt{\sqrt{\pi}2^n n!}}H_n(\xi)\exp\left[-\frac{1}{2}\xi^2\right] \quad \text{for } \xi=x_1-b'(t),$$

$$\Theta_n(x_1,t)=b''(t)x_1-\left(\frac{1}{2}+n\right)t+\frac{1}{2}\int[b'^2(t)-b''^2(t)]dt. \tag{40}$$

Here a constant phase factor has been omitted. Because of ρ=constant, the wave packet train described by R_n^2 in Eq. (40) keeps its shape in the temporary evolution. However, its center oscillates with coordinate $x_c=x_{1c}$, as in Eq. (34) generally or in Eq. (35) for the resonance case.

In the state $\psi_n=R_n e^{i\Theta_n}$, we calculate the expectation value of energy for the microscopic subsystem as Eq. (30). Applying Eqs. (32) and (37) to Eq. (30), we easily find the average energy

$$E_n(t)=\tfrac{1}{2}+n+\tfrac{1}{2}[p_{1c}^2(t)+x_{1c}^2(t)]+\lambda x_{1c}(t)\cos\nu t, \tag{41}$$

for $n=0,1,\ldots$. Here the first two terms are the quantum level of the harmonic oscillator, and the other terms constitute the classical energy in the form of Eq. (32). At $\lambda=0$ the classical energy is a constant and the average energy agrees with the quantum level after omitting a constant energy. Note that the corresponding macroscopic subsystem possesses the constant energy $E^{(0)}=\frac{1}{2}[\dot{x}_0^2(t)+x_0^2(t)]$, since it is a conservative system. On the other hand, for the instantaneous ground state of the microscopic subsystem, $n=0$, the quantum-mechanical expectation energy is equal to the corresponding classical energy after omitting the zero-point energy 1/2. This property is similar to that of the common coherent state of a harmonic oscillator. In fact, setting $\lambda=0$ and $n=0$, Eq. (40) is just in agreement with the well-known coherent state [12–14]. Therefore, we can call our wave function the generalized coherent state with multiple wave packets.

At the end of this section we emphasize that Eqs. (40) and (41) express the quantum-mechanical exact solutions of the driven oscillator system (32). In previous quantum mechanics [3], such a system was usually solved by using the quantum perturbation theory, where the driving field was treated as a perturbation. Obviously, our exact solutions completely differ from the previous quantum perturbed solutions, and there does not exist contradiction between them. In general, the perturbation theory is no longer valid in quantum mechanics, when the driving field is strong enough or too weak. The system under a microscopically strong field necessitates the exact solutions, and the system with a microscopically weak field requires the quantum perturbed solutions, where the driving fields are looked at as the classical fields. The very weak driving fields must be quantized by the scheme of quantum field theory and then are applied to the above-mentioned procedure, where the Fock representation may be more convenient [15,36].

In addition, from Eqs. (35) and (41) we know that in the resonance cases $\nu=\pm(E_{n+1}-E_n)=\pm 1(\omega)$, the wave packet center with coordinate $x_c=x_{1c}=x_{1,\nu=\pm 1}$ and the expectation value of energy will oscillate with infinite amplitude as time tending to infinity. This implies the resonance loss of stability for both the classical and quantum solutions, that may lead the system to transit to a state [37]. Thus we have proposed a method for studying the stabilities of quantum systems.

V. CHAOTIC COHERENT STATES OF A NONLINEAR OSCILLATOR

We have shown a kind of interesting CQC for the regular motions of a linear system, namely the particle wave packet correspondence in which the classical particle is the harmonic oscillator and the quantum wave packet is in the generalized coherent state of the harmonic oscillator. In this section, we are interested in suppressing the breakdown of the correspondence principle in the full quantum-mechanical treatment of a classical chaotic system [5–7]. We take the periodically driven Duffing oscillator with a macroscopic nonlinear potential and a microscopic periodic potential as an exemplification. The periodically driven Duffing oscillator model has many physical sources such as the magneto-elastic beams driven by an external periodic force [38,39], the Bose-Einstein condensate in a oscillating field [22,40] and so on. The macroscopic and microscopic potential of the model are written as [21,38,39]

$$V_0(x_0)=-\tfrac{1}{2}m\omega^2x_0^2+\tfrac{1}{4}\alpha x_0^4,$$

$$\lambda V_1(x_0,t)=\lambda x_0\cos\nu t \tag{42}$$

with α denoting the strength of nonlinearity. We will adopt the natural units $m=\hbar=\omega=1$ such that the space-time variables are normalized in units of the oscillator length $l_x=\sqrt{\hbar/(m\omega)}$ and inverse frequency ω^{-1}, respectively. Here a nonlinear term has been added compared to Eq. (31). So the functions $V_1'(t)$ and $V_0''(t)$ including the nonlinear effects read

$$V_0''(t)=\frac{\partial^2 V_0}{\partial x_0^2}=-1+3\alpha x_0^2(t),$$

$$V_1'(t)=\frac{\partial V_1}{\partial x_0}=\cos\nu t. \tag{43}$$

The corresponding macroscopic and microscopic Hamiltonians become

$$H_0=\frac{p_0^2}{2}-\frac{1}{2}x_0^2+\frac{1}{4}\alpha x_0^4,$$

$$H_1=\frac{p_1^2}{2}-\frac{1}{2}[1-3\alpha x_0^2(t)]x_1^2+\lambda x_1\cos\nu t. \tag{44}$$

Differing from the linear system, the microscopic Hamiltonian here directly depends on the classical solution $x_0(t)$. We well know that the macroscopic system governed by H_0 is nonchaotic and has several kinds of regular solutions, for example, the periodic solution and homoclinic one. The latter is associated with chaos of the microscopic subsystem in the sense of Smale's U-shaped transformation [41] under the Melnikov's chaos criterion [20,21]. For our purpose, we will employ the homoclinic solution $x_0(t)=x_h(t)$ of the macro-

scopic nonlinear oscillator to the microscopic Hamiltonian H_1 for demonstrating the CQC in the chaotic system.

The well-known homoclinic solution of the nonlinear oscillator dominated by H_0 in Eq. (44) reads [21,41]

$$x_0 = \sqrt{\frac{2}{\alpha}}\,\mathrm{sech}\,\tau, \quad \tau = t - \tau_0,$$

$$\tau_0 = t_0 - \mathrm{arcsech}\left(\sqrt{\frac{\alpha}{2}}x_0(t_0)\right), \tag{45}$$

where t_0 is the initial time and $x_0(t_0)$ the initial value of the macroscopic solution determined by the initial conditions. Note that the homoclinic solution describes the motion of the classical reference frame, there is no chaos in the reference frame thereby. Substituting Eq. (45) into the second of Eq. (44) produces the Hamiltonian

$$H_1 = \frac{p_1^2}{2} - \frac{1}{2}(1 - 6\,\mathrm{sech}^2\,\tau)x_1^2 + \lambda x_1 \cos\,\nu t. \tag{46}$$

Given Eq. (46), the Hamilton's canonical equations results in the classical equation

$$\ddot{x}_1 = [1 - 6\,\mathrm{sech}^2\,\tau]x_1 - \lambda\,\cos\,\nu t. \tag{47}$$

The homogenous equation of Eq. (47) with $\lambda = 0$ has the two linearly independent solutions [19,22]

$$\phi_1 = \dot{x}_0 = -\sqrt{\frac{2}{\alpha}}\,\mathrm{sech}\,\tau\tanh\,\tau,$$

$$\phi_2 = \phi_1 \int (\phi_1)^{-2}dt = \frac{3\sqrt{\alpha}}{2\sqrt{2}}\left(\tau\,\mathrm{sech}\,\tau\tanh\,\tau - \mathrm{sech}\,\tau + \frac{1}{3}\cosh\,\tau\right), \tag{48}$$

and the exact general solution of Eq. (47) can be expressed in terms of ϕ_1 and ϕ_2 as

$$x_{1c}(t) = \phi_1(t)\left(A + \lambda\int_0^t \phi_2(t)\cos\,\nu t dt\right) + \phi_2(t)\left(B - \lambda\int_0^t \phi_1(t)\cos\,\nu t dt\right),$$

$$p_{1c}(t) = \dot{\phi}_1(t)\left(A + \lambda\int_0^t \phi_2(t)\cos\,\nu t dt\right) + \dot{\phi}_2(t)\left(B - \lambda\int_0^t \phi_1(t)\cos\,\nu t dt\right), \tag{49}$$

which is similar to Eq. (9). The solution $(x_{1c}(t), p_{1c}(t))$ of Eq. (49) is bounded if and only if the condition

$$I_+ = B - \lambda\lim_{t\to\infty}\int_0^t \phi_1(t)\cos\,\nu t dt = 0 \tag{50}$$

is satisfied [19,22], because of $(\phi_2 \to \infty, \dot{\phi}_2 \to \infty)$ as time tending to infinity. The necessity of Eq. (50) can be easily seen by noticing the unboundedness of ϕ_2 at $t \to \infty$. Applying Eqs. (48) and (50) and the l'Hospital rule, one can calculate the superior and inferior limits of Eq. (49) as

$$\overline{\lim_{x\to\infty}}\, x_{1c}(t) = \overline{\lim_{x\to\infty}}\, p_{1c}(t) = \overline{\lim_{x\to\infty}}(\lambda\,\cos\,\nu t) = \lambda,$$

$$\underline{\lim_{x\to\infty}}\, x_{1c}(t) = \underline{\lim_{x\to\infty}}\, p_{1c}(t) = \underline{\lim_{x\to\infty}}(\lambda\,\cos\,\nu t) = -\lambda. \tag{51}$$

This just supplies proof on the sufficiency of Eq. (50). In the calculation, the constant B is determined by Eq. (50).

An interesting result is that Eqs. (50) and (48) infer the formula $I_- = B - \lambda\int_0^{-\infty}\phi_1(t)\cos\,\nu t dt = B - \lambda\,\cos\,\nu\tau_0\int_0^{-\infty}\phi_1(\tau)\cos\,\nu\tau d\tau = I_+ = 0$ for $\sin[\nu\tau_0(t_0)] = 0$. From $(I_+ - I_-)/\lambda = 0$ we arrive at the Melnikov's chaos criterion [20]

$$M(t_0) = \int_{-\infty}^{\infty}\phi_1(t)\cos\,\nu t dt = \sqrt{2}\pi\nu\,\sin[\nu\tau_0(t_0)]\mathrm{sech}\,\frac{\pi\nu}{2} = 0 \tag{52}$$

for some t_0 values. Here $M(t_0)$ is the Melnikov function, which measures the distance between the stable and unstable manifolds in the Poincare section at t_0. The simple zero of Eq. (52) indicates the existence of chaos [42,43]. Applying $\nu\tau_0 = j\pi$ to Eq. (45) we get the initial condition for chaos as

$$x_0(t_0) = \sqrt{\frac{2}{\alpha}}\,\mathrm{sech}\left(t_0 - j\frac{\pi}{\nu}\right), \quad j = 0, 1, \ldots\ . \tag{53}$$

We call the solution (49) obeying the chaos criterion (52) the "chaotic solution" [19]. Combining Eqs. (48) with (49) we perceive that the final term of the solution x_{1c} consists of an unbounded function $\phi_2(t)$ and an analytically unsolvable integration, which cannot be expressed by the finite numbers of elementary functions. In the procedure of numerically simulating the time evolution of Eq. (49), the small deviations from the unsolvable integration are unavoidable, due to any computer cannot calculate the infinite terms. But any infinitesimal deviation will destroy the boundedness condition (50) and will be amplified exponentially rapid by the function $\phi_2(t)$. Therefore, the chaotic solution is analytically unsolvable and numerically uncomputable so that it is unpredictable. Although precisely predicting chaotic orbit is impossible, making use of Eq. (51) we can determine the position and momentum of the Duffing oscillator to a microscopic interval, $(x_{1c}, p_{1c}) \in [-\lambda, \lambda]$ with widths $\Delta x_{1c} = \Delta p_{1c} = 2\lambda$ for any sufficiently large time.

Our main tasks are to derive the quantum-mechanical exact solution of the chaotic oscillator from the above-mentioned procedure, and reveal the corresponding quantum chaotic properties. Applying the known functions $\phi_i(t)$ in Eq. (48) to the CQC condition of Eq. (28) gives the solutions of Eq. (13)

$$\varphi_1 = \sqrt{c_0}\phi_1(t), \quad \varphi_2 = \sqrt{c_0}\phi_2(t). \tag{54}$$

Combining this equation with Eqs. (16), (17), and (20)–(22), we obtain the solutions of Eq. (12) as

$$c = \frac{1}{2}\dot{\theta} - i\frac{\dot{\rho}}{2\rho}, \quad \rho = \sqrt{c_0(\phi_1^2 + \phi_2^2)},$$

$$\theta = \arctan\frac{\phi_2}{\phi_1} = \arctan\left[\frac{3\alpha}{4}\left(\coth\tau - \tau - \frac{1}{3}\cosh^3\tau\, csch\,\tau\right)\right],$$

$$e = \pm\frac{\sqrt{c_0}}{\rho}, \quad f = \pm\frac{\rho b'}{\sqrt{c_0}}, \tag{55}$$

$$b' = \frac{\sqrt{c_0}\phi_1}{\rho^2}\left(b_0' + \lambda\sqrt{c_0}\int_0^t \phi_2 \cos\nu t dt\right) + \frac{\sqrt{c_0}\phi_2}{\rho^2}\left(b_0'' - \lambda\sqrt{c_0}\int_0^t \phi_1 \cos\nu t dt\right),$$

$$b'' = \frac{\sqrt{c_0}\phi_1}{\rho^2}\left(b_0'' - \lambda\sqrt{c_0}\int_0^t \phi_1 \cos\nu t dt\right) - \frac{\sqrt{c_0}\phi_2}{\rho^2}\left(b_0' + \lambda\sqrt{c_0}\int_0^t \phi_2 \cos\nu t dt\right),$$

$$a_n = \frac{c_0^{1/4}}{\sqrt{\sqrt{\pi}2^n n!\rho(t)}}\exp\left\{-i\left[\left(\frac{1}{2}+n\right)\theta - \frac{1}{2}\int (b'^2 - b''^2)dt\right]\right\}. \tag{56}$$

Here functions $\phi_i(t)$ are given in Eq. (48). Inserting Eqs. (55) and (56) into Eq. (25) can get the evident form of the chaotic wave function, which is of the generalized coherent state (not shown here). Examining Eq. (25) we find that the norm of the wave function represents a train of Gaussian wave packets with the width and height being proportional to $\rho(t)$ and $\rho^{-1}(t)$, respectively. That is, the deformations of wave packets are described by the function $\rho(t)$, which is deterministic in Eq. (55) with Eq. (48). Using Eqs. (29) and (56) and the formulas $b_0'/\sqrt{c_0}=A, b_0''/\sqrt{c_0}=B$, we obtain the expectation value $x_{1q}(t)=x_{1c}(t)$ of x_1 and the center position $x_c(t)=x_{1c}(t)$ of the wave packet train in the form of Eq. (49), whose value is unpredictable in the chaotic region $[-\lambda,\lambda]$.

In Fig. 1(a), we show the time evolution of the quantum expectation value $x_{1q}(t)$ from Eqs. (49) and (48), where the parameter set $\alpha=A=\mu=1$, $\tau_0=0$, $\lambda=0.1$, $B=\lambda\lim_{t\to-\infty}\int_0^\infty\phi_1(t)\cos\nu t dt=-0.020\,975$ has been used to plot the curve. The corresponding phase orbit is plotted as in Fig. 1(b). Here the black parts are the sketch maps of the chaotic region $x_{1q}\in[-\lambda,\lambda]=[-0.1,0.1]$, $p_{1q}\in[-\lambda,\lambda]=[-0.1,0.1]$ in which the quantum state cannot be exactly determined. Substituting Eqs. (49) and (48) into Eq. (30) produces the expected energy $E_n(t)$ of the chaotic state, which depends on the classical chaotic solution and the function $\rho(t)=\sqrt{c_0(\phi_1^2+\phi_2^2)}$. Therefore, such quantum level is also unpredictable for a long time, as shown in Fig. 2.

Asymptotic behavior of the chaotic state is very interesting, since Eqs. (48), (55), and (56) mean that

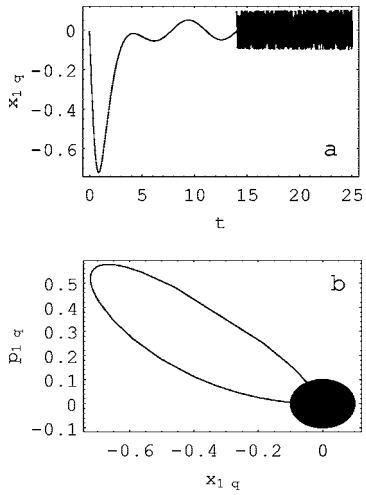

FIG. 1. (a) The time evolution of the quantum expectation coordinate $x_{1q}(t)=x_{1c}(t)$ from Eqs. (49) and (48) for the parameter set $\alpha=A=\mu=1$, $\tau_0=0$, $\lambda=0.1$, $B=-0.020\,975$. The chaotic system becomes unpredictable at about $t=14$. (b) The phase orbit of $x_{1q}(t)$, $p_{1q}(t)$ for the same parameters with (a). The black circle is the sketch map of the chaotic region in the phase space. The space-time coordinates have been normalized in units of $l_x=\sqrt{\hbar/(m\omega)}$ and ω^{-1}, respectively.

$$\lim_{t\to\infty}\rho(t) = \lim_{t\to\infty}\dot{\rho}(t) = \infty, \quad \lim_{t\to\infty}\theta = -\frac{\pi}{2},$$

$$\lim_{t\to\infty} a_n = \lim_{t\to\infty} b' = \lim_{t\to\infty} b'' = 0. \tag{57}$$

Inserting them into Eq. (30) and noticing Eqs. (43), (45), and (51), the asymptotic energies are evaluated as

$$\overline{\lim_{x\to\infty}} E_n(t) = \overline{\lim_{x\to\infty}}\left[\tfrac{1}{2}(p_{1c}^2 - x_{1c}^2) + \lambda\cos(\nu t)x_{1c}\right] = \tfrac{3}{2}\lambda^2,$$

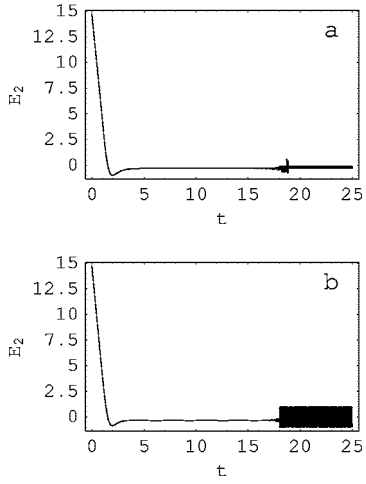

FIG. 2. The time evolution of the expected energy E_n in the chaotic state $\psi_n(x_1,t)$ for the parameters $n=2$, $c_0=1$, $\alpha=A=\mu=1$, $\tau_0=0$, $B=-0.020\,975$, and (a) $\lambda=0.1$, (b) $\lambda=1$. The energy and time are in units of $\hbar\omega$ and ω^{-1}. The thick lines after $t=17$ are the sketch maps of the chaotic regions of energy with the width $\Delta E=3\lambda^2$.

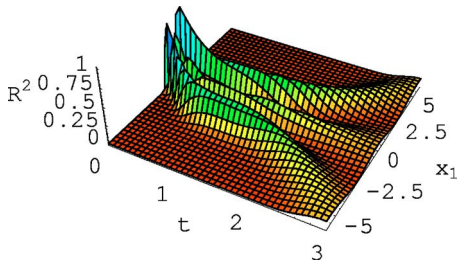

FIG. 3. (Color online) The space-time distribution of the chaotic probability density $R_n^2(x_1,t)$ for $n=2$, $c_0=1$ and $\alpha=A=\mu=1$, $\tau_0=0$, $\lambda=0.1$, $B=-0.020\,975$. The probability density is in units of l_x^{-1} and the space-time coordinates are normalized in units of $l_x=\sqrt{\hbar/(m\omega)}$ and ω^{-1}.

$$\lim_{x\to\infty} E_n(t) = \lim_{x\to\infty}\left[\tfrac{1}{2}(p_{1c}^2 - x_{1c}^2) + \lambda\cos(\nu t)x_{1c}\right] = -\tfrac{3}{2}\lambda^2, \tag{58}$$

which are independent of the quantum number n. This result exhibits the chaotic region of energy, $\left[-\frac{3}{2}\lambda^2, \frac{3}{2}\lambda^2\right]$ with width $\Delta E=3\lambda^2$, and implies that chaos may suppress the quantum effect of energy. The chaotic region of energy has been hinted as the thick lines in Fig. 2 for (a) $\lambda=0.1$ and (b) $\lambda=1$, respectively.

The space-time distribution of the chaotic probability density $R_n^2(x_1,t)$ is shown by the three-dimensional plot as in Fig. 3. It can be clearly seen from this figure that the nonzero probability distribution exists only in the space-time region $x_1\in(-5,5), t\in(0,3)$. The probability density decays to zero for the spatial variable outside the region and $t>3(\omega^{-1})$. In fact, adopting the asymptotic values of Eq. (57) to Eq. (25) shows that at $t\to\infty$ the wave packets described by the norm of wave function will collapse to the waves of zero height and infinite width, however, the normalization condition is still valid and the expectation values of physical quantities can be nonzero and finite. These properties are similar to that of the normalized plane wave $\sqrt{L^{-1}}e^{ix}$ with normalization constant L being an infinite spatial distance. The chaotic wave, of course, differs from the plane wave. Its center plays chaotic oscillations as time tends to infinity, and the expectation values of the coordinate, momentum and energy fall in some small regions and cannot be predicted precisely.

VI. CONCLUSIONS AND DISCUSSIONS

We have proposed a mathematically consistent protocol for investigating the macroscopic-microscopic coupled system. Applying the classical perturbation theory and treating the microscopic interactions as the perturbations, we separate the system into the macroscopic reference frame and microscopic subsystem. The classical and quantum exact solutions of the microscopic subsystems are constructed, which contain the quantum chaotic coherent state corresponding to the classically chaotic solution, while the macroscopic reference frame moves along the classical homoclinic orbit. The good classical-quantum correspondences are found in the microscopic subsystems through their exact solutions. The regular and chaotic quantum states and levels, and the quantum chaotic regions are revealed in the systems exemplified by the periodically driven linear oscillator and nonlinear Duffing system. The results show that chaos may cause the collapse of matter wave packets and suppress the quantum effect of energy.

For the quantum wave packets describing the microscopic subsystem, the width, height, and center-of-mass motion depend on the classical solutions of the subsystem. This implies that the microscopic subsystems in different quantum states associated with different classical solutions possess different features of motion. We well know that any classical solution is determined by the initial conditions of the classically treated subsystem. The latter are related to the arbitrary constants A and B in Eq. (9). Therefore, how to prepare and detect experimentally the quantum states by adjusting the classical initial conditions becomes quite an interesting and important problem. However, the classical initial conditions concern the initial coordinate and momentum, which cannot be set and controlled precisely in quantum mechanics, because of the Heisenberg uncertainty relation. Particularly, the classical and quantum chaotic states are unpredictable even for the given initial conditions, although we have derived the chaotic regions and revealed some chaotic features. These difficulties and challenges deserve further investigations.

ACKNOWLEDGMENTS

This work was supported by the National Natural Science Foundation of China under Grant No. 10275023, and by the Laboratory of Magnetic Resonance and Atomic and Molecular Physics of China.

[1] A. Einstein, Ann. Phys. **17**, 891 (1905).
[2] P. Roman, *Advanced Quantum Theory* (Addison-Wesley, New York, 1965).
[3] Y. Zhang, *Quantum Mechanics* (Science Press, Beijing, 2002) (in Chinese).
[4] G. Wenzel, Z. Phys. **38**, 518 (1926); H. M. Kramers, *ibid.* **39**, 828 (1926); L. Brillouin, C. R. Acad. Sci. URSS, Ser. A **183**, 24 (1926).
[5] T. Hogg and B. A. Huberman, Phys. Rev. Lett. **48**, 711 (1982); Phys. Rev. A **28**, 22 (1983); S. Chandrasekhar, Rev. Mod. Phys. **15**, 1 (1943).
[6] R. Roncaglia, L. Bonci, B. J. West, and P. Grigolini, Phys. Rev. E **51**, 5524 (1995).
[7] B. S. Helmkamp and D. A. Browne, Phys. Rev. Lett. **76**, 3691 (1996).
[8] L. E. Reichl, *The Transition to Chaos in Conservative Classical Systems: Quantum Manifestations* (Springer-Verlag, New York, 1992).

[9] F. Haake, *Quantum Signatures of Chaos* (Springer-Verlag, New York, 1992).
[10] J. Gong and P. Brumer, Phys. Rev. A **68**, 062103 (2003).
[11] A. K. Pattanayak and P. Brumer, Phys. Rev. Lett. **77**, 59 (1996).
[12] E. Schrödinger, Naturwiss. **14**, 664 (1926).
[13] S. Howard and S. K. Ray, Am. J. Phys. **55**, 1109 (1987).
[14] J. R. Klauder and B. Skagerstam, *Coherent states* (World Scientific, Singapore, 1985).
[15] L. S. Brown, Phys. Rev. Lett. **66**, 527 (1991).
[16] W. Hai, S. Huang, and K. Gao, J. Phys. B **36**, 3055 (2003).
[17] M. M. Nieto and D. R. Truax, New J. Phys. **2**, 18 (2000); Phys. Rev. Lett. **71**, 2843 (1993).
[18] G. G. Athanasiu and E. G. Floratos, Nucl. Phys. B **425**, 343 (1994).
[19] W. Hai, Y. Duan, and L. Pan, Phys. Lett. A **234**, 198 (1997); W. Hai *et al.*, J. Phys. A **31**, 2991 (1998); Phys. Lett. A **275**, 54 (2000); W. Hai, X. Zhang, W. Huang, and G. Chong, Int. J. Bifurcation Chaos Appl. Sci. Eng. **11**, 2263 (2001).
[20] V. K. Melnikov, Trans. Mosc. Math. Soc. **12**, 1 (1963).
[21] Z. Liu, *Perturbation Criteria for Chaos* (Shanghai Scientific and Technological Education Press, Shanghai, 1994) (in Chinese).
[22] W. Hai, Y. Xiao, J. Fang, W. Huang, and X. Zhang, Phys. Lett. A **265**, 128 (2000); C. Lee, W. Hai, and L. Shi, Phys. Rev. A **64**, 053604 (2001); W. Hai, Z. Zhang, and J. Fang, Eur. Phys. J. B **21**, 103 (2001); W. Hai, C. Lee, G. Chong, and L. Shi, Phys. Rev. E **66**, 026202 (2002); G. Chong, W. Hai, and Q. Xie, *ibid.* **70**, 036213 (2004); Chaos **14**, 217 (2004); J. Fang, W. Hai, G. Chong, and Q. Xie, Physica A **349**, 133 (2005).
[23] B. R. Holstein and J. F. Donoghue, Phys. Rev. Lett. **93**, 201602 (2004).
[24] H. Schomerus and J. Tworzydlo, Phys. Rev. Lett. **93**, 154102 (2004).
[25] A. Anderson, Phys. Rev. Lett. **74**, 621 (1995); **76**, 4090 (1996); K. R. W. Jones, *ibid.* **76**, 4087 (1996); L. Diósi, *ibid.* **76**, 4088 (1996); I. R. Senitzky, *ibid.* **76**, 4089 (1996).
[26] L. Diósi and J. J. Halliwell, Phys. Rev. Lett. **81**, 2846 (1998).
[27] J. Rasmussen, Nucl. Phys. B **582**, 649 (2000).
[28] For instance, see C. Meier, Phys. Rev. Lett. **93**, 173003 (2004); J. Gong, and P. Brumer, *ibid.* **88**, 203001 (2002); M. P. de Miranda and F. J. Aoiz, *ibid.* **93**, 083201 (2004); L. E. Ballentine, Phys. Rev. A **70**, 032111 (2004); W. Boucher and J. Traschen, Phys. Rev. D **37**, 3522 (1988); D. Rossini, G. Benenti, and G. Casati, Phys. Rev. E **70**, 056216 (2004).
[29] M. Born, W. Heisenberg, and P. Jordan, Z. Phys. **35**, 557 (1925).
[30] E. Schrödinger, Ann. Phys. **80**, 437 (1926).
[31] W. Hai, M. Feng, X. Zhu, L. Shi, K. Gao, and X. Fang, Phys. Rev. A **61**, 052105 (2000); W. Hai, X. Zhu, M. Feng, L. Shi, K. Gao, and X. Fang, J. Phys. A **34**, L79 (2001).
[32] Y. Gu, *Quantum Chaos* (Shanghai Science Technical Press, Shanghai, 1996) (in Chinese).
[33] M. C. Gutzwiller, *Chaos in Classical and Quantum Mechanics* (Springer-Verlag, New York, 1990).
[34] K. Husimi, Prog. Theor. Phys. **9**, 381 (1953).
[35] W. Hai, C. Lee, and G. Chong, Phys. Rev. A **70**, 053621 (2004).
[36] D. Leibfried, R. Blatt, C. Monroe, and D. Wineland, Rev. Mod. Phys. **75**, 281 (2003).
[37] L. F. Landovitz, Phys. Rev. A **11**, 67 (1975).
[38] P. J. Holmes, Philos. Trans. R. Soc. London, Ser. A **292**, 419 (1979).
[39] F. C. Moon and P. J. Holmes, J. Sound Vib. **65**, 275 (1979); F. C. Moon, ASME J. Appl. Mech. **47**, 638 (1980).
[40] F. Kh. Abdullaev and R. A. Kraenkel, Phys. Rev. A **62**, 023613 (2000).
[41] B. Liu and J. Peng, *Nonlinear Dynamics* (Advanced Education Publishing House, Beijing, 2004) (in Chinese).
[42] R. Chacón and J. I. Cirac, Phys. Rev. A **51**, 4900 (1995).
[43] M. Bartuccelli, P. L. Christiansen, N. F. Pedersen, and M. P. Soerensen, Phys. Rev. B **33**, 4686 (1986).